Physico-chemical removal of heavy metals from contaminated water using recyclable montmorillonite cellulose nanocomposite

D. Abunah[1]*, C. Onindo[1], D. Andala[2], E. Ochoti[1]

[1]Department of Chemistry, Kenyatta University, P.O Box 43844-00100 Nairobi, Kenya
[2]Department of Chemistry, Multimedia University, P.O Box 15653-00503 Nairobi, Kenya

Abstract

Most studies have focused on economic and efficient remediation of water polluted with toxic metals using adsorbents. However, very little attention is paid on the fate of the spent adsorbents. The present work aimed at fabricating a nanocomposite adsorbent by intercalating cellulose molecules into the interlayer spacing of sodic-montmorillonite clay. The adsorbent was thereafter characterized comprehensively by X-ray diffraction (XRD), Fourier transform infrared spectroscopy (FTIR), Scanning electron microscope (SEM) and surface area measurement by Brunauer-Emmett-Teller (BET) isotherm studies. Batch studies were carried out to determine the influence of adsorption parameters. The data obtained from batch experiments had highest agreement with Freundlich isotherm. The adsorption capacities (K_f) were 16.1 mg/g and 11.1 mg/g for the adsorption of Cu (II) and Cd (II) ions, respectively. Pseudo second order model gave the best fit with the experimental data. From thermodynamic studies, the negative values of Gibbs free energy (ΔG^o) and enthalpy change (ΔH^o) indicate that the adsorption process was spontaneous and exothermic, respectively. The negative values of ΔS^o indicate that the adsorption process resulted into reduced randomness at the solid/liquid interface. Aqueous ammonia exhibited the best regeneration efficiency over HCl, EDTA and NaOH eluents. The results indicate that MMT cellulose nanocomposite material has a great potential for use in water remediation strategies.

1. Introduction

A large fraction of the world's population has little access to clean water [28]. For example, Kenya with an approximate population of 50 million people, about 43 % of this population cannot access clean and safe drinking water. The main factors contributing to this scarcity include; droughts, deforestation, rapid population growth, industrialization and poor management of water supplies [21]. The quality of water is compromised by the presence of contaminants and one such contaminant is toxic heavy metals. Heavy metals are generally emitted during their mining and processing. Domestic and municipal application of metals and their compounds have also introduced substantive amounts of toxic metals into the environment. These heavy metals cause serious toxic effects to humans, animals and plants [7]. Due to the foresaid ubiquitous nature of these metals, the pollution by metals is thus considered as one of the high risk pollution that must be monitored and reduced to within allowable concentrations in the environment.

Many water treatment techniques have been applied to remove toxic metals from wastewater [11]. These methods principally include: chemical precipitation, reverse osmosis (RO), flotation, membrane filtration and ion-exchange. However, these methods have serious limitations such as production of toxic sludge [1]. Furthermore, the listed methods are less effective when the concentrations of metal ions are in trace levels [19]. These inefficiencies have led to the development of alternative removal techniques and one such technique is development of modified clays as an adsorbent. The current work proposed to deal with the fabrication and application of a recyclable MMT cellulose nanocomposite for remediation of water contaminated by Cu (II) and Cd (II) ions.

2. Materials and Methods

2.1. Sampling and extraction of montmorillonite clay (MMT clay)

The montmorillonite clay that was used in the current study was extracted from depths between 20 to 50 cm below ground level from Kamwana village whose global positioning system (GPS) is ($0°19'4.404''S$, $35°1'17.004''E$), of Nyakach sub-county in Kenya. The extraction site was identified by looking for cracked surface because according to Gidigasu and Gawu [12], cotton clays crack during dry spells and swells when moistened.

2.2 Chemicals, apparatus and instruments

2.2.1 Chemicals

The chemicals used in this study were of analytical grade, they were purchased from Sigma Aldrich. They included; copper (II) sulphate pentahydrate, cadmium (II) nitrate tetrahydrate, sodium chloride, sodium hydroxide, hydrochloric acid, ethylene diamine tetra-acetic acid (EDTA), aqueous ammonia, silver nitrate, urea, thiourea and polyvinyl alcohol (PVA).

2.2.2 Apparatus and instruments

The XRD diffractograms of the materials were taken by SCINTAG XDS- 2000 POWDER DIFFRACTOMETER, the surface topographical features were taken by SEM (Hitachi S-3400N). Water samples were shaken on a digital reciprocating shaker (WiseShake SHR-2D model). Surface functionality was analyzed by FTIR (IRTracer-100 model). The surface areas determined by BET (Micrometric ASAP 2020 analyzer model) and the residual metal ions quantified by AAS (Shimadzu AA-6300 model). Other equipments include; weighing balance (ATX 224 SHIMADZU), oven (WTC binder), grinding mill (Retsch SR 200 rotor beater mill), pH meter (OHAUS STARTER 2000), centrifuge (DM0412), shaking water bath (KOTTERMANN LABORTECHNIK) and deep freezer (MIKA model).

2.3 Nanocomposite preparation

2.3.1 Cleaning of the extracted montmorillonite clay

Two kilograms of the extracted MMT clay was dispersed in two litres of distilled water, the mixture was stirred for twenty minutes. The suspension thereafter poured into a thick cotton bag and hanged to allow water to drip for 72 hours.

2.3.2 Conversion of cleaned MMT clay into sodic form

Two litres of 1.0 M NaCl were added to the cleaned MMT clay and stirred for twenty minutes. The clay suspension then poured into a thick cotton bag and hanged to allow water to drip for 72 hours. Fresh 1.0 M NaCl were added to the residue, stirred for twenty minutes and poured into a thick cotton bag and hanged to allow water to drip for another 72 hours. The sodium saturated MMT clay was washed by adding two litres of distilled water, stirring for twenty minutes and the resultant suspension poured into a thick cotton bag and hanged to allow water to drip for 72 hours, this washing with distilled water and dripping was repeated up to the third wash when there was negative test for chloride ions when tested with silver nitrate [23].

2.3.3 Solvent extraction of cellulose from cotton wool

The solvent was prepared by mixing water, urea, sodium hydroxide and thiourea in the ratio 77:8:8:7. The mixture was stirred to dissolve the solid chemicals. Twenty grams of cotton wool were then soaked into the solvent. The beaker then transferred into a deep freezer at -10 $°$C and left to stand at that temperature overnight. The beaker was removed from the deep freezer the following day and placed in the sun to melt down part of its contents. The contents of the beaker were poured on a sieve that was placed onto another beaker and the contents on the sieve squeezed with a glass rod so as to collect liquid content in the beaker. The liquid collected in the beaker contained dissolved cellulose as was tested using HCl acid: shorter fibers reappeared when drops of hydrochloric acid were added into a small sample of the collected liquid [29].

2.3.4 Fabrication of the nanocomposite

Twenty grams of polyvinyl alcohol (PVA) were added into two litres of cold distilled water and the PVA allowed to hydrate in this water for two hours, then a gradual warming up to 90 $°$C and gentle stirring for twenty minutes to dissolve PVA. The entire sodic MMT clay then added into the PVA solution and stirred for a further twenty minutes at 90 $°$C. The extracted cellulose were added into the PVA-clay mixture and stirring continued for another twenty minutes at the same temperature. The hot suspension obtained then allowed to cool and its pH adjusted to 7 using 0.1 M HCl acid and thereafter poured into a thick cotton bag and hanged to allow water to drip for 72 hours. The resultant residue was sun dried for one sunny day then oven dried at 100 $°$C overnight. The oven dried

material was pulverized and sieved using 100 μm mesh wire and the sieved material was used in characterization, batch experiments and batch washing experiments.

2.4 Batch experiments

In an attempt to investigate a given parameter, that parameter was varied while keeping the other parameters constant. The residual metal ions were quantified by AAS. The amount adsorbed (q_e) and the percentage removal were then calculated using equations 1 and 2, respectively [9]:

$$q_e = \frac{(C_o - C_e)}{m} \times V \tag{1}$$

$$\% \text{ Removal} = \frac{(C_o - C_e)}{C_o} \times 100 \tag{2}$$

Where, q_e is the adsorbed amount at equilibrium (mgg^{-1}), C_o and C_e are the metal concentration (mgL^{-1}) before and after adsorption, respectively, m is the mass of adsorbent used (gram) and V being the volume of solution used in each experiment (litres)

2.5 Batch washing experiments (Adsorbent regeneration)

Batch washing experiments were conducted to determine the regeneration capability of spent adsorbent using; 0.1 M EDTA, 0.1 M NaOH, 0.1 M aq. ammonia and 0.1 M HCl acid as the eluents. Eighty milligram samples of the nanocomposite material were added into contaminated water samples and the experimental conditions were: temperature: 25 ± 2 °C, pH: 4, shaking time: 60 minutes, dosage: 80 mg/50 ml, Cu (II) ions concentration: 20 mg/L and shaking speed: 170 rpm. The solutions were thereafter transferred into empty bottles for AAS analysis. The adsorbents were further shaken at 170 rpm for 20 minutes with the respective eluents followed by shaking the regenerated adsorbents at 170 rpm in distilled water for another 20 minutes. Nineteen more adsorption-desorption cycles were conducted to determine the regeneration efficiency of the nanocomposite.

3. Results and discussion

3.1 Characterization of the adsorbents

3.1.1 Fourier transform infrared spectroscopy (FTIR)

The surface functionality of the nanocomposite material was verified by FTIR analysis and the FTIR spectrum reported in figure 1.
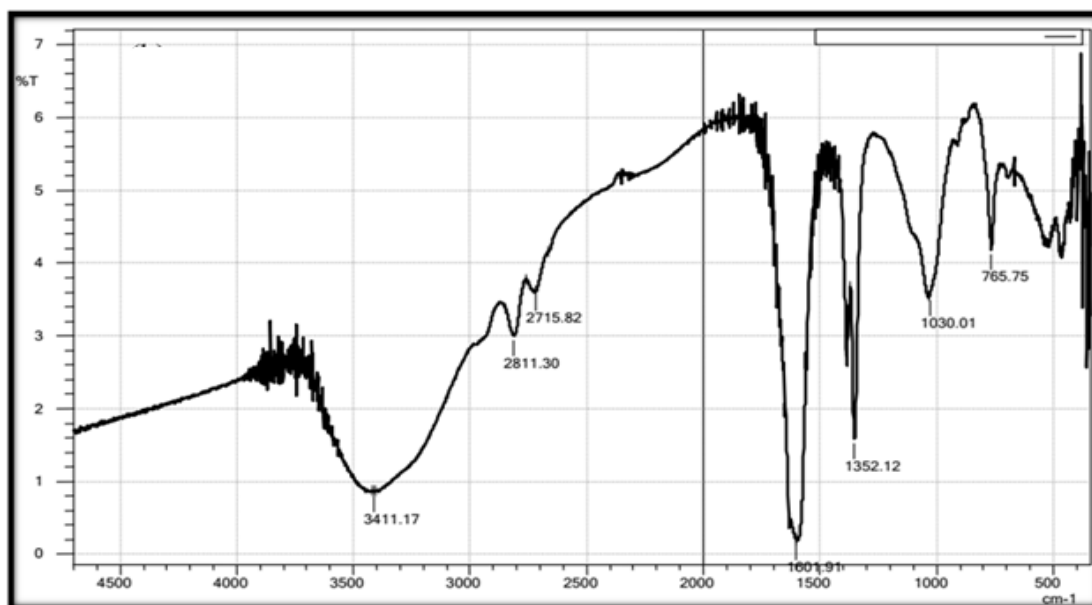

Figure 1: FTIR spectrum of MMT cellulose nanocomposite material

The strong and broad absorption band at 3,411.17 cm^{-1} is ascribed to -OH bond stretching vibrations; the -OH groups whose absorption band is reported herein is due to oxygen atoms which are not used in bonding together the clay layers. While the band at 765.75 cm^{-1} is attributed to surface hydroxyl bond bending vibrations. The weak absorption bands appearing at 2,811.30 and 2,715.82 cm^{-1} was attributed to C-H bond stretching vibrations. The

band at 1,601.91 cm^{-1} is for C=O bond stretching vibrations. The band at 1,030.01 cm^{-1} was assigned to Si-O bond stretching vibrations of siloxane (Si-O-Si) in the tetrahedral sheet of clay. The band at 1,352.12 cm^{-1} was assigned to Al-O bond stretching vibrations [17]. The observed absorption bands indicate that the adsorbent material has chemical functional groups on its surface such as; carbonyl and hydroxyl which help in the binding of metal ions.

3.1.2 Surface area measurement
The BET specific surface areas, average pore diameters and pore volumes of MMT clay and MMT cellulose nanocomposite were summarized and reported in table 1.

Table 1: BET surface area and pore properties of MMT clay and MMT cellulose nanocomposite

Sample	BET surface area (m^2/g)	Pore volume (cm^3/g)	Average pore diameter (nm)
MMT Clay	59.4679	0.066573	4.47792
MMT cellulose nanocomposite	10.3606	0.023546	9.09043

Montmorillonite clay had a specific surface area of 59.4679 m^2/g. Upon intercalation of cellulose molecules into its galleries, the surface area reduced to 10.3606 m^2/g. A similar trend was observed in a voltammetric examination of smectite clays by Ngameni *et al.* [23] . The pore volume also showed a similar trend by decreasing from, 0.066573 cm^3/g to 0.023546 cm^3/g upon intercalation of polymer molecules into the interlayer spacing of MMT clay. However, the average pore diameter of MMT clay was 4.47792 nm and increased to 9.09043 nm upon intercalation of polymer molecules into the interlayer spacing of MMT clay. The inverse relationship between surface area/pore volume and pore diameter could be due to the filling and blocking of some pores on clay by molecules with larger pore diameters. Larger diameter of pores allows for only a smaller number of pores fitting within a set of total volume of material. The pores are the responsible factor for exposed surface area; low porosity materials have low exposed surface. Similar trends were reported in previous studies by Lim *et al.* [18]

3.1.3 XRD analysis
The X-ray diffraction patterns of MMT clay and MMT cellulose nanocomposite were taken and reported in figures 2 (a) and (b), respectively. The X-ray diffraction pattern of MMT clay showed sharp prominent peaks at 2θ values at 21.062⁰, 26.846⁰ and 28.229⁰ (figure 2 a). These sharp peaks indicate that the MMT clay mineral that was used in this study had a well defined crystalline structure [24]. The d-spacing of the materials were calculated from the 2θ based on Bragg's equation given by equation 3:

$$d = \frac{n\lambda}{2Sin\theta}$$
(3)

Where, d is the space between the layers, θ is the measured diffraction angle, λ is the wavelength of X-ray used, n is an integer, representing the order of reflection. The calculated d-spacing of montmorillonite clay for the prominent peaks at 21.062⁰, 26.846⁰ and 28.229⁰ were 2.14 Å, 1.70 Å and 1.62 Å, respectively.

The MMT cellulose nanocomposite showed prominent sharp peaks at 2θ values at 20.934⁰, 26.707⁰ and 27.555⁰ (figure 2 b). The sharp pointed peaks indicate that the MMT cellulose nanocomposite formed had a well defined crystalline structure [24]. Equation 3 was used to determine the d-spacing of MMT cellulose nanocomposite. The calculated d values were reported as; 2.16 Å, 1.72 Å and 1.67 Å for the peaks at 2θ values at 20.934⁰, 26.707⁰ and 27.555⁰, respectively. The d-spacing increased upon formation of MMT cellulose nanocomposite. This was as a result of intercalation of cellulose molecules into the MMT clay galleries. The increased d-spacing is evident by comparing the calculated d values of MMT clay (2.14 Å, 1.70 Å and 1.62 Å) with the corresponding d values of MMT cellulose nanocomposite (2.16 Å, 1.72 Å and 1.67 Å). Further to the increased d values, several minor peaks that crowded on the original MMT clay (figure 2 a) disappeared when MMT cellulose nanocomposite was formed (figure 2 b), this suggests an extensive expansion of basal spacing resulting into exfoliation of clay platelets [24].
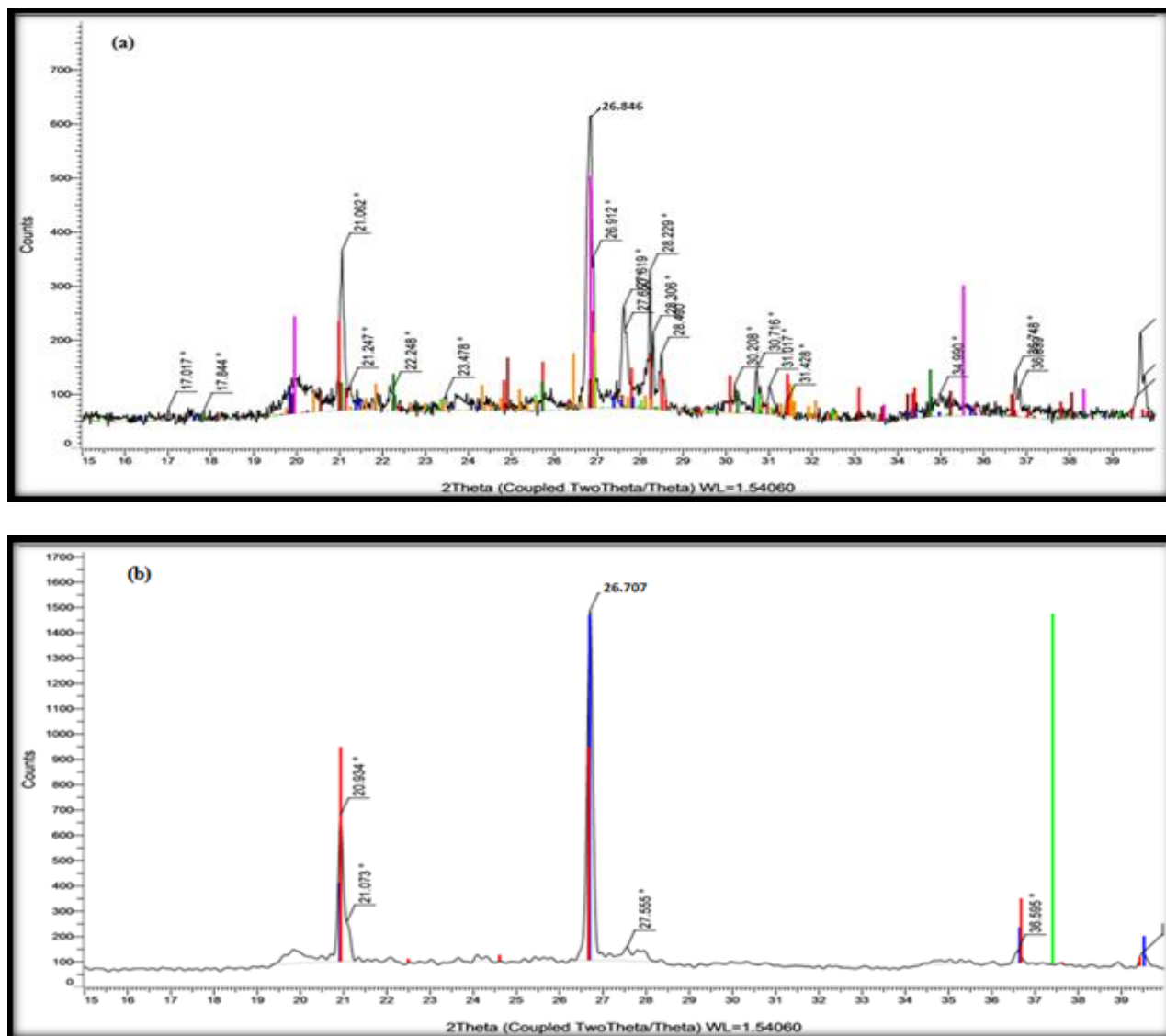
Figure 2: XRD spectra of MMT clay (a) and MMT cellulose nanocomposite (b)

3.1.4 Surface morphology of MMT clay and MMT cellulose nanocomposite

The surface morphology of MMT clay and MMT cellulose nanocomposite were analyzed by SEM imaging. Figures 3 (a) and (b) reports the results of SEM images at 10 magnification

Figure 3 (a) shows that montmorillonite clay exhibited a comparatively rough surface while figure 3 (b) indicates that MMT cellulose nanocomposite prepared by intercalation of cellulose molecules into the MMT clay galleries showed a rather smooth but comparatively densely populated surface despite having been crushed into uniform size distribution of 100 μm as the MMT clay. The pores of MMT clay are larger than those of the MMT cellulose nanocomposite, because the intercalated cellulose molecules filled and blocked some of the pores that were originally on MMT clay and a new pore system was formed. Equally, the deposition of molecules onto the surface of MMT clay as it forms MMT cellulose nanocomposite resulted into increased population of molecules on the material (figures 3 b).

3.2 Adsorption studies

3.2.1 Effect of adsorbent dosage on the adsorption of Cu (II) and Cd (II) ions

This parameter was investigated by varying the adsorbent mass from 20, 80, 140, 200, 260 and 320 mg. Each experiment was done in triplicate, the average values worked out and the analyzed results were reported in figure 4. There was an increase in the percentage removal of Cu (II) ions ranging from 89.73 % to 99.01 % with optimum percentage removal being at a dosage of 80 mg. For Cd (II) ions, the percentage removal increased from 86.3 % to 99.23 % with optimum percentage removal at a dosage of 140 mg. The percentage removal decreased thereafter as the adsorbent mass was further increased for both metal ions. These trends are consistent with the findings by Das *et al.* [8] in their study on the removal of copper using alluvial soil of India.
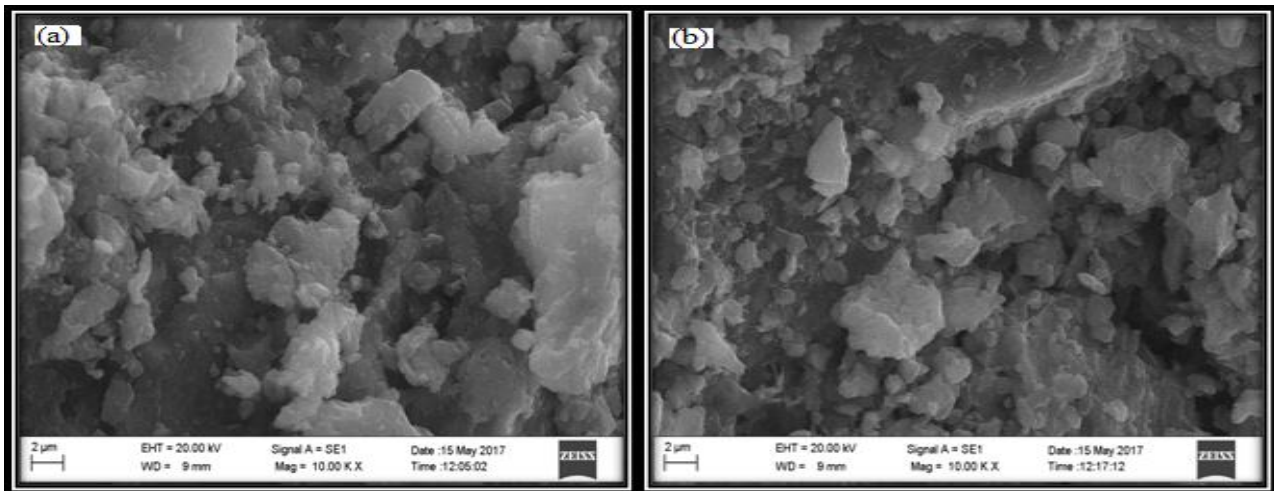
Figure 3: SEM photomicrographs of MMT clay (a) and MMT cellulose nanocomposite (b) both at 10 magnification
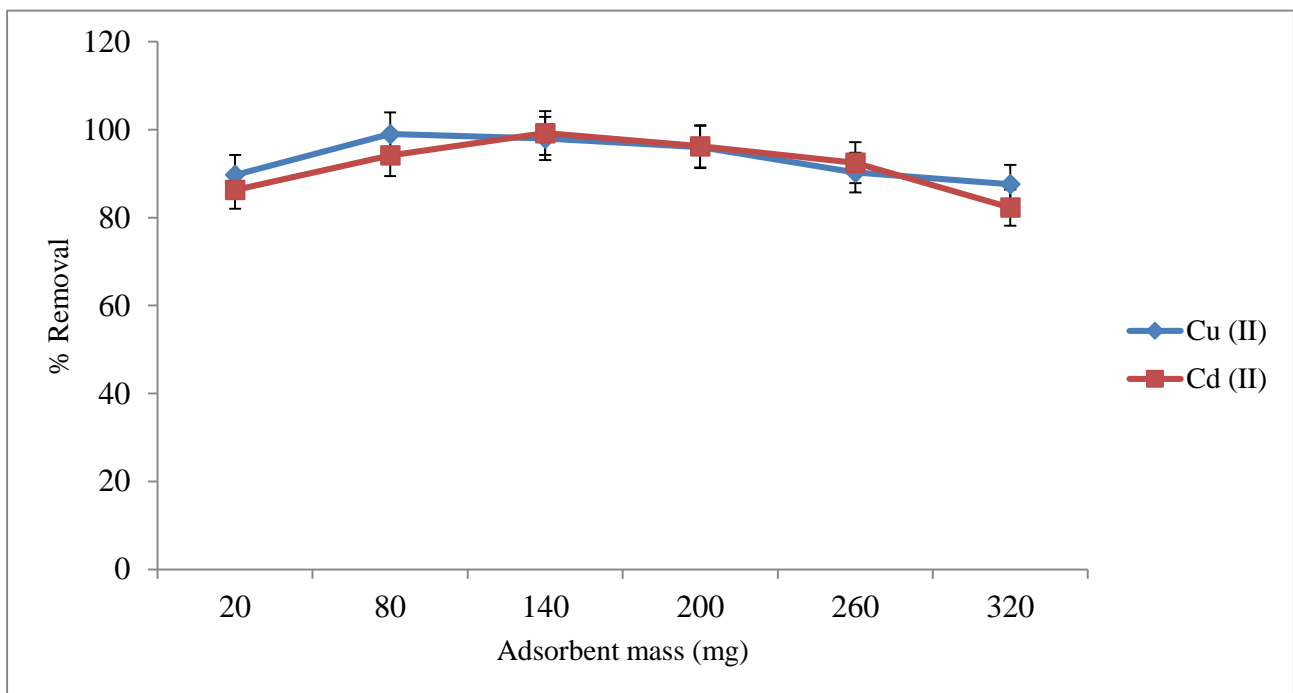

Figure 4: Effect of adsorbent dosage on adsorption of Cu (II) and Cd (II) ions by MMT cellulose nanocomposite (initial metal ion concentration: 10 mg/L, time: 120 minutes, temperature: 25 ± 2 °C, pH: 6, shaking speed: 170 rpm)

The lower removal efficiency at lower adsorbent mass is caused by the saturation of the adsorbent particles by the metal ions. Adsorption capacity increased as the adsorbent mass was increased to an optimum adsorbent dosage at; 80 mg and 140 mg for Cu (II) and Cd (II) ions, respectively. The increased adsorption capacity is attributed to the increasing number of vacant adsorptive sites due to increasing surface area at higher mass of the adsorbent [2]. The percentage removal declined when the dosage was increased further. This decline in adsorption at higher adsorbent mass is caused by the overlapping or aggregation of vacant adsorptive sites: the charged particles on the adsorbent surfaces start interacting at higher adsorbent mass hence causing hindrance to adsorption [5].

3.2.2 Effect of pH on the adsorption of Cu (II) and Cd (II) ions
This parameter was studied by varying the pH of contaminated water from 2, 3, 4, 5, 6 to 7. Each experiment on the effect of pH was done in triplicate and the analyzed data reported in figure 5. The percentage removal of Cu (II) ions ranged from 74.76 to 98.37 %, while that of Cd (II) ions ranged from 64.14 to 92.12 %. The MMT cellulose nanocomposite had a high percentage removal over a range of pH values from 4 to 6 with the highest removal being at a pH = 4. These trends are in agreement with the trends observed by Ahamed and Begum [4] who studied adsorption of copper using low cost adsorbent.
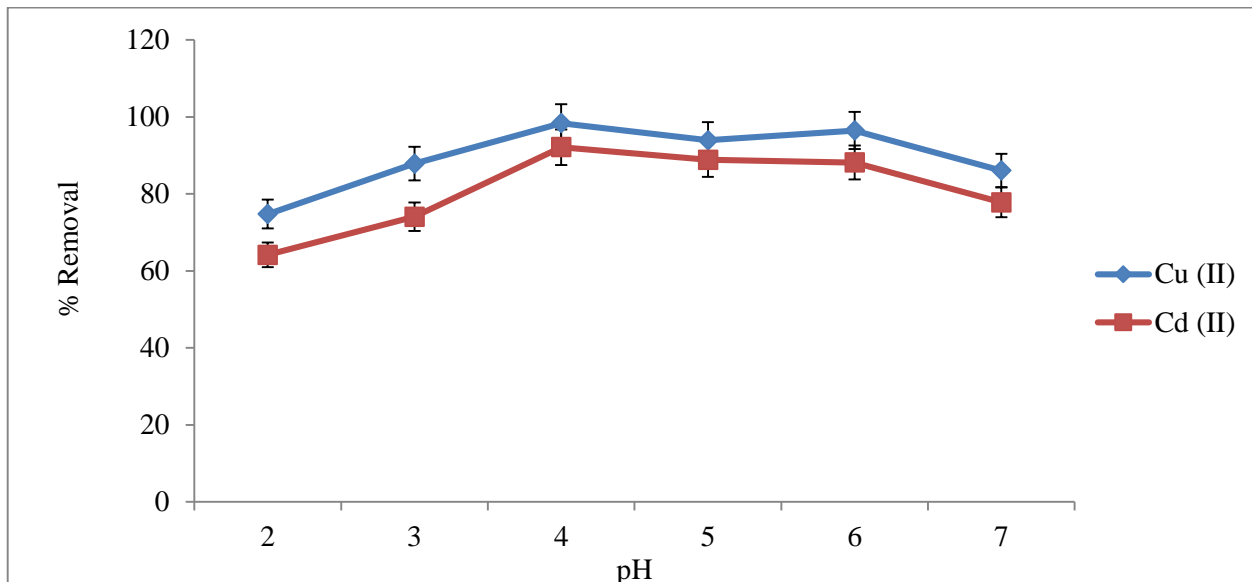
Figure 5: Effect of pH on the adsorption of Cu (II) and Cd (II) ions by MMT cellulose nanocomposite (initial ion concentration: 10 mg/L, time: 120 minutes, temperature: 25 ± 2 °C, dosage: 80 mg and 140 mg for Cu (II) and Cd (II) ions, respectively and shaking speed: 170 rpm)

Adsorption of metal ions was comparatively less favorable at lower pH values since at pH lower than 4, the binding sites are highly protonated and this causes a strong competition for the binding sites between the protons and the metal ions. Furthermore, the presence of high number of protons at lower pH values reduces the affinity of adsorptive sites on the nanocomposite material for the metal ions. This is due to increased hindrance to diffusion of metal ions caused by the increasing cation-cation repulsive forces [4]. At moderate pH values (pH of 4 to 6), the adsorbent is relatively more negatively charged than the bulk solution and this contributes to the increased affinity for metal ions at pH values from 4 [27]. Higher pH (pH > 7) were not used in the current study to avoid the removal of metal ions by precipitation [9].

3.2.3 Effect of initial metal ion concentration on the adsorption of Cu (II) and Cd (II) ions
Metal ion concentration was varied from 10, 20, 100, 200, 400 to 500 mg/L while keeping other parameters constant. Each experiment was done in triplicate and filtered samples quantified by AAS. The percentage removal were worked out from the AAS results and reported in figure 6. From the results, the initial concentration has an effect on the uptake efficiency of MMT cellulose nanocomposite.
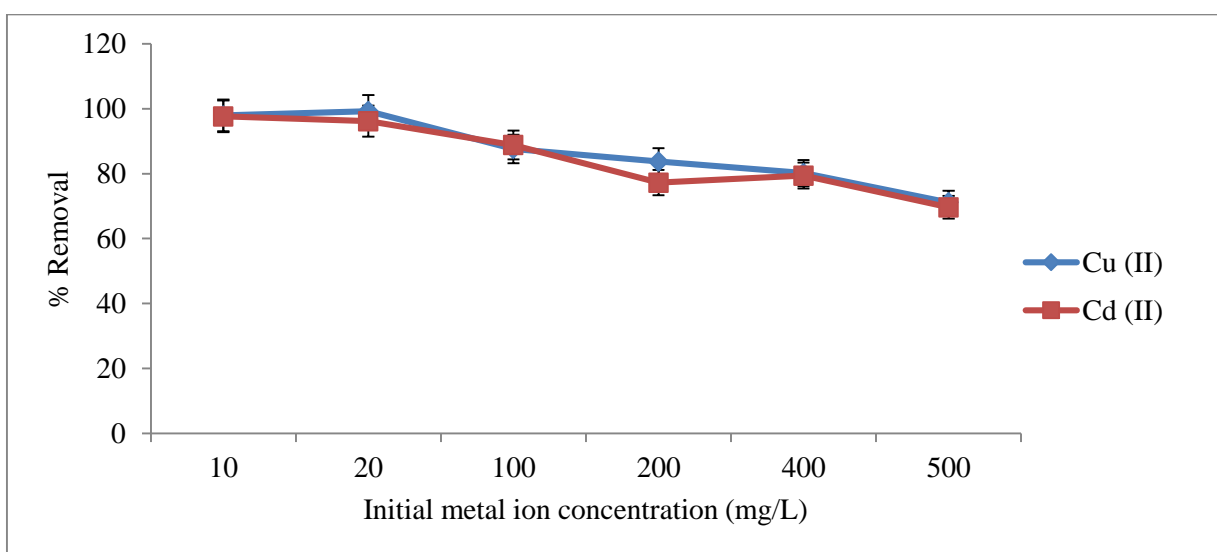

Figure 6: Effect of initial concentration on the adsorption of Cu (II) and Cd (II) ions by MMT cellulose nanocomposite (temperature: 25 ± 2 °C, time: 120 minutes, pH: 4.0, dosage: 80 and 140 mg for Cu (II) and Cd (II) ions, respectively and shaking speed: 170 rpm)

The optimum percentage removal of both Cu (II) and Cd (II) ions occurred at 20 mg/L. At this optimum initial concentration, 99.27 % and 96.2 % of Cu (II) and Cd (II) ions were adsorbed, respectively. As initial concentration was further increased, the amount adsorbed increased but the percentage removal dropped from 99.27 % to 71.17 % and 96.2 % to 69.64 % for Cu (II) and Cd (II) ions, respectively. A similar trend was observed for the removal of Zn (II), Cu (II), Cd (II) and Pb (II) ions by biosorbents [6,3]. It may be concluded that the MMT cellulose nanocomposite has a highest adsorption capacity at lower concentrations of Cu (II) and Cd (II) ions. This is because, at lower concentrations, the adsorptive surfaces are less saturated by metal ions. An increase in the adsorbed amount of metal ions as initial metal ion concentration was increased was observed, this is due to the increased driving force of the concentration gradient. Adsorption capacity of the MMT cellulose nanocomposite thereafter reduced as the concentration of the metal ions were increased further to much higher concentrations; this is due to the decreasing number of adsorptive surfaces as a result of saturation of these surfaces by metal ions at higher concentrations [10].

3.2.4 Effect of contact time on the adsorption of Cu (II) and Cd (II) ions

The effect of time was investigated by varying time from 5, 15, 25, 35, 60 to 120 minutes while keeping temperature, pH, initial ion concentration and adsorbent dosage constant. Each experiment was done in triplicate, the average values were worked out and the analyzed data presented in figure 7. The adsorption of Cu (II) and Cd (II) ions increased drastically up to 15th minute then became gradual from 15th to 35th minutes and thereafter the adsorption became constant for both metal ions used in this study. A similar trend was observed by Jiang *et al.* [16] in their study of Cd $^{2+}$, Cu $^{2+}$, Pb $^{2+}$ and Ni $^{2+}$ sorption onto kaolinite clay.
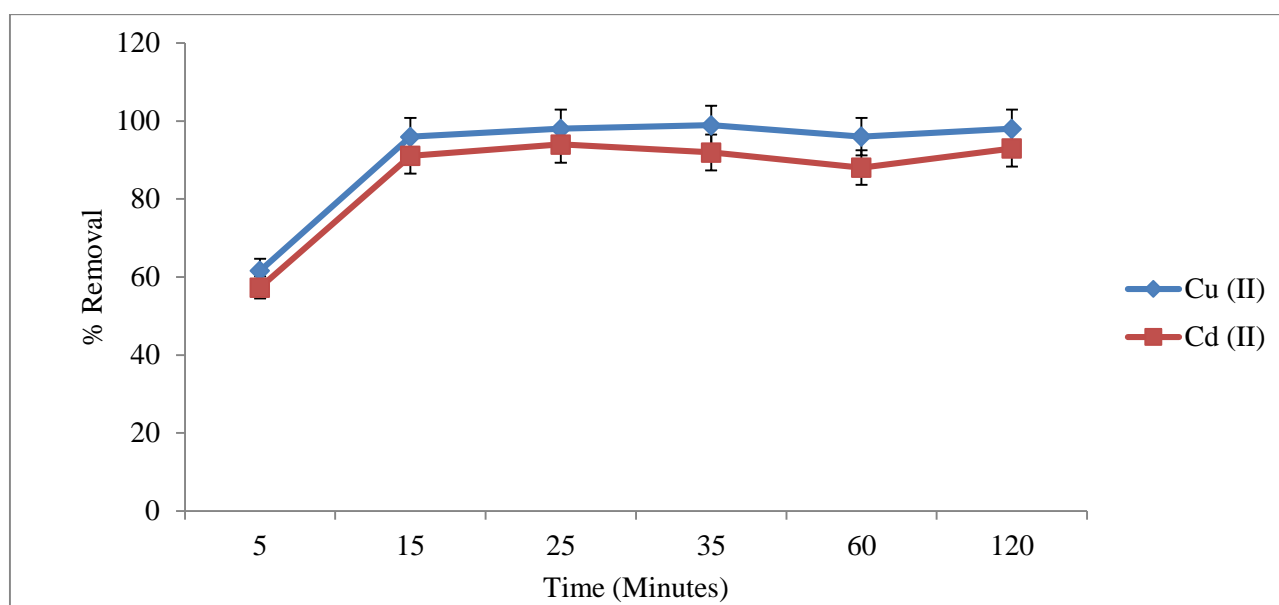

Figure 7: Effect of contact time on the adsorption of Cu (II) and Cd (II) ions by MMT cellulose nanocomposite (temperature: 25 ± 2 °C, initial ion concentration: 20 mg/L, pH: 4.0, dosage: 80 mg and 140 mg for Cu (II) and Cd (II) ions, respectively and shaking speed: 170 rpm)

The rapid increase in percentage removal at the beginning of the adsorption process is due to the high number of vacant adsorptive surfaces on MMT cellulose nanocomposite and this result into a higher solute concentration gradient [15]. High solute concentration gradient results into a faster diffusion of metal ions to the adsorbent surface, this is occasioned by the resultant stronger driving force. With passage of time, that is at about 15th to 35th minutes, the adsorptive surfaces become saturated with metal ions and further adsorption becomes difficult as a result of repulsion between the adsorbed ions on the adsorbent material with those in the bulk solution. After 35th minute, the vacant adsorptive surfaces become highly populated with adsorbed metal ions. These adsorbed metal ions repel the oncoming metal ions that are supposed to adsorb onto the adsorbent surface and hence hindering adsorption [25].

3.2.5 Effect of temperature on the adsorption of Cu (II) and Cd (II) ions

The percentage removal of Cu (II) and Cd (II) ions by MMT cellulose nanocomposite was studied as a function of temperature with contact time, pH, initial ion concentration and adsorbent mass being kept constant. The temperature was varied from 20, 30, 40, 50 to 60 °C. Each experiment on the effect of temperature was done in

triplicate, average values were worked out and the analyzed data reported in figure 8. The removal of Cu (II) and Cd (II) ions was highest at lower temperatures with a percentage removal of 97.02 % and 94.51 % for Cu (II) and Cd (II) ions, respectively at 20 °C. On further increase in temperature, the percentage adsorbed decreased steadily from 97.02 to 80.7 % for Cu (II) ions and 94.51 to 72.7 % for Cd (II) ions. Mahmoud and El-Halwany [20] observed a similar trend in their study of adsorption of cadmium onto orange peels.
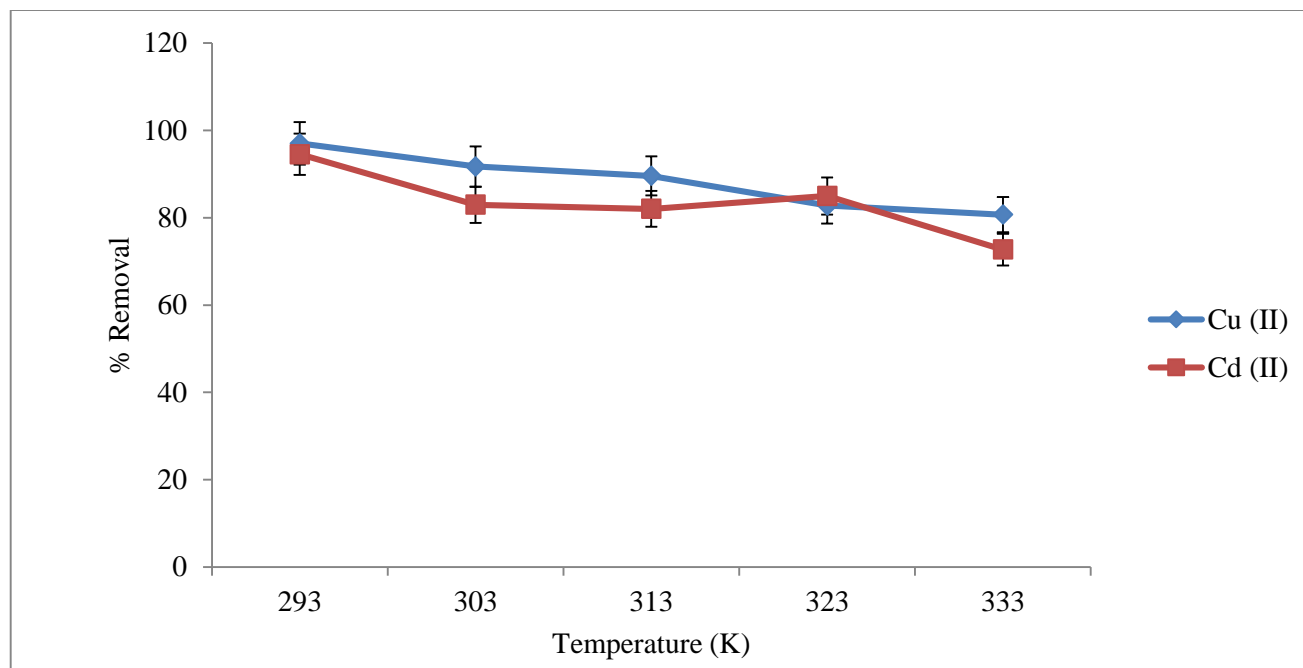

Figure 8: Effect of temperature on the adsorption of Cu (II) and Cd (II) ions by MMT cellulose nanocomposite (initial ion concentration: 20 mg/L, time: 120 minutes, pH: 4.0, dosage: 80 mg and 140 mg for Cu (II) and Cd (II) ions, respectively and shaking speed: 170 rpm)

The percentage removal of Cu (II) and Cd (II) ions decreased with increase in temperature, that is; higher temperatures worked against the adsorption of Cu (II) and Cd (II) ions. Declining adsorption capacity of the nanocomposite material with increase in temperature is due to the weakening of the bonds holding metal ions onto the adsorptive surfaces of the nanocomposite material. Increase in temperature also causes deterioration of the matrix structure of the nanocomposite material thereby resulting into loss of some adsorptive sites, hence reducing the removal efficiency for Cu (II) and Cd (II) ions. The decrease in adsorption efficiency as temperature was increased suggest a weak binding interactions between the adsorptive surfaces and the cations; this is an indicator that the process could be exothermic and therefore leading to the conclusion that the adsorption process was favorable at lower temperatures [22].

3.3 Adsorption isotherms
Langmuir and Freundlich isotherms are widely applied due to their simplicity and ability to fit into most of the experimental data. The parameters of these isotherms provide the adsorbent's adsorption capacity [14]. The parameters of Langmuir and Freundlich modeling were worked out and reported in Table 2. The MMT clay and MMT cellulose nanocomposite exhibited near equal adsorption capacities for the adsorption of Cu (II) and Cd (II) ions with nanocomposite showing a slight drop in adsorption for Cu (II) ions and a much improved adsorption capacity for Cd (II) ions as indicated in table 2. The extremely low K_f value of 4.136 mg/g for MMT clay reported for the adsorption of Cd (II) ions requires speciation study to determine the species of cadmium ions present and this could explain the huge deviation from the other K_f values reported herein.
The R^2 values for Freundlich and Langmuir isotherms fit for the adsorption of Cu (II) ions onto MMT cellulose nanocomposite were 0.907 and 0.956, respectively. Similar R^2 values for the adsorption of Cd (II) ions were 0.931 and 0.992, respectively as indicated in table 2. By comparing the R^2 values, the Freundlich isotherm had a strong correlation to the experimental data: this indicates that the adsorption of Cu (II) and Cd (II) ions onto MMT cellulose nanocomposite was multilayer. From the Freundlich model, $\frac{1}{n}$ values are less than 1 indicating that the adsorption process was favorable. The adsorption capacities (K_f) found to be 16.1 mgg⁻¹ and 11.1 mgg⁻¹ for the adsorption of Cu (II) and Cd (II) ions, respectively.

Table 2: Isotherm model parameters for Cu (II) and Cd (II) ions adsorption on MMT clay and MMT cellulose nanocomposite

Isotherm model	Model parameters	Parameter values for the adsorption of Cu (II) ions on		Parameter values for the adsorption of Cd (II) ions on	
		MMT cellulose Nanocomposite	MMT Clay	MMT cellulose Nanocomposite	MMT Clay
Freundlich	K_f (mg/g)	16.1	17.354	11.1	4.136
	$\frac{1}{n}$	0.481	0.4899	0.557	0.7118
	R^2	0.956	0.9645	0.992	0.9674
Langmuir	Q_{max} (mg/g)	200	178.57	142.857	181.82
	b (dm^3/g)	0.04348	0.08875	0.066	0.017
	R^2	0.907	0.975	0.931	0.9456

3.4 Kinetics study

Pseudo first and second order models were used to analyze the kinetics data. Table 3 reports the kinetic parameters for the adsorption of the metal ions by MMT cellulose nanocomposite

Table 3: Parameters of pseudo first and second order kinetic models

Kinetic model	Model parameters	Parameter values for the adsorption of Cu (II) ions	Parameter values for the adsorption of Cd (II) ions
Pseudo first order	K_1(min^{-1})	0.00691	0.0115
	q_e (mgg^{-1})	0.6	0.3
	R^2	0.218	0.106
Pseudo second order	K_2 ($gmg^{-1}min^{-1}$)	0.0563	0.1632
	q_e^2 (mgg^{-1})	5.102	4.6948
	R^2	0.993	0.998

The calculated q_e values for pseudo second order rate model were relatively closer to the experimental q_e values reported in table 3. But in the case of pseudo first order rate model, the calculated q_e values were not in par with experimental values. This trend was equally supported by a strong correlation coefficient (R^2) in pseudo second order rate model unlike pseudo first order rate model where R^2 values are lower indicating weak correlation between experimental and theoretical data. An adsorption process which is best described by pseudo second order model is based on the assumption that the rate determining step is the chemical coordination step (metal-adsorbent reactions). This suggests that the adsorption process involves two species that is metal ions and the active sites. In such an adsorption process which obeys pseudo second order model; film, pore and bulk diffusions are faster than the metal-adsorbent coordination reactions which takes place at the active sites [14].

3.5 Thermodynamic study

The thermodynamic parameters such as; enthalpy change (ΔH^o), entropy change (ΔS^o) and Gibbs free energy (ΔG^o) are important in determining the nature of adsorption process. The values of ΔS^o and ΔH^o were obtained from the intercept and slope, respectively of Van't Hoff plot. The computed thermodynamic parameters were summarized and reported in table 4. The negative sign on ΔG^o values indicate that the adsorption process for both Cu (II) and Cd (II) ions was spontaneous. The ΔG^o values became less negative with increasing temperature, this suggest that the adsorption of the metal ions became less spontaneous at higher temperatures. Increase in temperature causes deterioration of the matrix structure of the nanocomposite and this leads to loss of adsorptive surfaces, hence reducing the removal efficiency for the metal ions. The enthalpy changes (ΔH^o) were negative for both Cu (II) and Cd (II) ions suggesting that the adsorption process was exothermic in nature. From table 4, the absolute enthalpy changes were; 40.456 k J/mol and 29.639 kJ/mol for the adsorption of Cu (II) and Cd (II) ions, respectively. These absolute values are within a range which indicates that the adsorption of Cu (II) and Cd (II) ions were physico-chemical rather than being purely chemical or physical [26,13]. Entropy changes (ΔS^o) were negative indicating reduced randomness at the solid/liquid interface. The randomness reduced at the solid/liquid interface due to the adsorption of the metal ions which resulted into firming of these metal ions onto the adsorbent surface.

Table 4: Adsorption thermodynamic parameters at different temperatures

Adsorbate	Temperature (K)	ΔG^o (kJ/mol)	ΔH^o (kJ/mol)	ΔS^o (J/mol/K)
Cu (II)	293 303 313 323 333	- 6.796 - 4.308 - 3.794 - 2.356 - 2.041	- 40.456	- 116.811
Cd (II)	293 303 313 323 333	- 5.243 - 2.243 - 2.145 - 2.794 - 0.792	- 29.639	- 86.2161

3.6 Desorption Studies (Adsorbent regeneration)

The adsorbents were regenerated by batch washing in a large excess of eluents and the regenerated adsorbents were reused up to twenty cycles of adsorption with Cu (II) ions as the adsorbate; these high number of adsorption cycles were undertaken to determine the efficiency of the nanocomposite at higher adsorption cycles. The findings were summarized and reported in figures 9 (a) and (b). The efficiency of the regenerated MMT cellulose nanocomposite ranged between 99 to 94 %, 91 to 60 %, 40 to 7 % and 97 to 85 % when aq. NH_3, HCl, EDTA and NaOH were used, respectively as eluents.
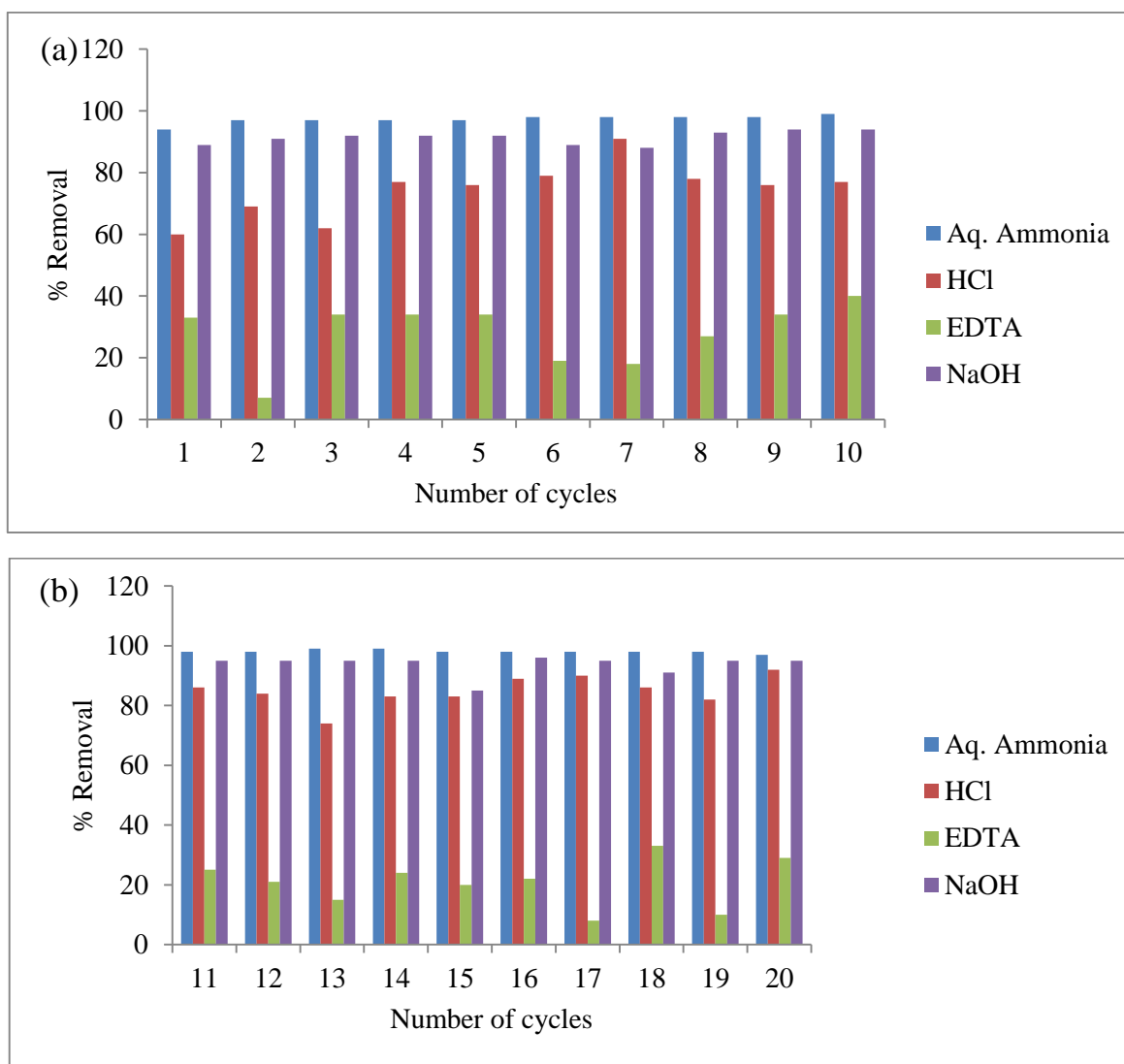
Figure 9: 1st to 10th adsorption cycles (a) and 11th to 20th adsorption cycles (b)

The alkaline solutions of 0.1 M aqueous ammonia and 0.1 M sodium hydroxide gave much better and near equal efficiency for the regeneration of MMT cellulose nanocomposite as compared to 0.1 M solutions of HCl acid and EDTA. On comparison, 0.1 M aqueous ammonia exhibited much better regeneration efficiency for the nanocomposite than the other three eluents, because aqueous ammonia forms a complex ion with copper (II) ions (tetraammine Cu (II) complex). The formation of this complex ion enhances the interaction and solubility of Cu (II) ions into aqueous ammonia. The efficiency of MMT cellulose nanocomposite did not exhibit a significant decrease as shown in figure 9 when aqueous ammonia was used as the eluent. The MMT cellulose nanocomposite material is both acid and base resistant and it has an excellent potential for reuse.

Conclusion

Findings herein show that the adsorption by the nanocomposite was optimal at; pH: 4, time: 35 minutes, adsorbent mass: 80 and 140 mg for Cu (II) and Cd (II) ions, respectively, initial concentration: 20 mg/L and at lower temperatures. The equilibrium data best fitted Freundlich isotherm and adsorption capacity of the nanocomposite for Cu (II) and Cd (II) ions being 16.1 and 11.1 mg/g, respectively. The kinetics data best fitted pseudo second order model indicating that the metal-adsorbent reaction was the rate determining step. The ΔG^o values became less negative as temperature was increased indicating that the adsorption process was more spontaneous at lower temperatures. The ΔH^o values were negative indicating that the adsorption was exothermic and the absolute values of ΔH^o reported suggest that the adsorption was physico-chemical in nature. Aqueous ammonia exhibited the best regeneration efficiency for the spent nanocomposite. The findings in the present study indicate that, fabricated MMT cellulose nanocomposite material has a great potential for use in water remediation strategies. This is supported by the fact that the nanocomposite has a high adsorption capacity and it can be used up to many adsorption cycles.

References

1. A. Aadil, M. Munir, A. Faiza, N. Sumera, Z. Amna, Removal of Chromium (VI) by biosorption using different agricultural byproducts of some important cereal crops as biosorbents, *Middle East Journal of Scientific Research,* 6 (2010) 512-516.
2. N. Abdel-Ghani, M. Hefny, G. A. El-Chaghaby, Removal of lead from aqueous solution using low cost abundantly available adsorbents, *International Journal of Environmental Science and Technology,* 4 (2007) 67. https://doi.org/10.1007/BF03325963
3. S. Abdel-Halim, A. Shehata, M. El-Shahat, Removal of lead ions from industrial waste water by different types of natural materials, *Water Research,* 37 (2003) 1678-1683. https://doi.org/10.1016/S0043-1354(02)00554-7
4. A. J. Ahamed, A. S. Begum, Adsorption of copper from aqueous solution using low-cost adsorbent, *Archives of Applied Science ResearcH,* 4 (2012) 1532-1539.
5. N. R. Bishnoi, M. Bajaj, N. Sharma, A. Gupta, Adsorption of Cr (VI) on activated rice husk carbon and activated alumina, *Bioresource technology,* 91 (2004) 305-307. https://doi.org/10.1016/S0960-8524(03)00204-9
6. P. A. Brown, J. M. Brown, S. J. Allen, The application of kudzu as a medium for the adsorption of heavy metals from dilute aqueous wastestreams, *Bioresource technology,* 78 (2001) 195-201. https://doi.org/10.1016/S0960-8524(00)00144-9
7. G. Crini, Recent developments in polysaccharide-based materials used as adsorbents in wastewater treatment, *Progress in polymer science,* 30 (2005) 38-70. https://doi.org/10.1016/j.progpolymsci.2004.11.002
8. B. Das, N. Mondal, R. Bhaumik, P. Roy, K. Pal, C. Das, Removal of copper from aqueous solution using alluvial soil of Indian Origin: Equilibrium, kinetic and thermodynamic study, *Journal of Material and Environmental Science,* 4 (2013) 392-409.
9. F. Dawodu, G. Akpomie, M. Ejikeme, P. Ejikeme, The use of Ugwuoba clay as an adsorbent for zinc (II) ions from solution, *International Journal of Multidisciplinary Sciences and Engineering,* 3 (2012) 13-18.
10. E. Fourest, J. C. Roux, Heavy metal biosorption by fungal mycelial by-products: Mechanisms and Influence of Ph, *Applied Microbiology and Biotechnology,* 37 (1992) 399-403. https://doi.org/10.1007/BF00211001
11. F. Fu, Q. Wang, Removal of heavy metal ions from wastewaters: A Review, *Journal of environmental management,* 92 (2011) 407-418. https://doi.org/10.1016/j.jenvman.2010.11.011

12. S. Gidigasu, S. Gawu, The mode of formation, nature and geotechnical characteristics of black cotton soils, A Review, *Standard Scientific Research and Essays,* 14 (2013) 377-390.

13. I. H. Gubbuk, Isotherms and thermodynamics for the sorption of heavy metal ions onto functionalized sporopollenin, *Journal of hazardous materials,* 186 (2011) 416-422. https://doi.org/10.1016/j.jhazmat.2010.11.010

14. R. Herrero, P. Lodeiro, R. Rojo, A. Ciorba, P. Rodríguez,M. E. S de Vicente, The efficiency of the red alga mastocarpus stellatus for remediation of cadmium pollution, *Bioresource technology,* 99 (2008) 4138-4146. https://doi.org/10.1016/j.biortech.2007.08.065

15. M. M. Ibrahim, W. W. Ngah, M. Norliyana, W. W. Daud, M. Rafatullah, O. Sulaiman, R. Hashim, A novel agricultural waste adsorbent for the removal of lead (II) ions from aqueous solutions, *Journal of hazardous materials,* 182 (2010) 377-385. https://doi.org/10.1016/j.jhazmat.2010.06.044

16. M. Q. Jiang, X. Y. Jin, X. Q. Lu, Z. I. Chen, Adsorption of Pb (II), Cd (II), Ni (II) and Cu (II) onto natural kaolinite clay, *Desalination,* 252 (2010) 33-39. https://doi.org/10.1016/j.desal.2009.11.005

17. V. Kanchana,T. Gomathi, V. Geetha, P. Sudha, Adsorption analysis of Pb (II) by nanocomposites of chitosan with methyl Cellulose and clay, *Der Pharmacia Lettre,* 4 (2012) 1071-1079.

18. S. Lim, S. H. Yoon, Y. Shimizu, H. Jung, I. Mochida, Surface control of activated carbon fiber by growth of carbon nanofiber, *Langmuir,* 20 (2004) 5559-5563.

19. P. Lodeiro, J. Barriada, R. Herrero, M. S. De Vicente, The marine macroalga cystoseira baccata as biosorbent for cadmium (II) and lead (II) removal: Kinetic and equilibrium studies, *Environmental pollution,* 142 (2006) 264-673. https://doi.org/10.1016/j.envpol.2005.10.001

20. M. A. Mahmoud, M. M. El-Halwany, Adsorption of cadmium onto orange peels: Isotherms, kinetics, and thermodynamics, *Journal of Chromatography and Separation Techniques,* 5 (2014) 1. http://dx.doi.org/10.4172/2157-7064.1000238

21. S. Marshall, The water crisis in Kenya: Causes, effects and solutions, *Global Majority E-Journal,* 2 (2011) 31-45.

22. L. Mataka, S. Salidu, W. Masamba, J. Mwatseteza, Cadmium sorption by moinga stenopetala and moringa oleifera seed powder, *International Journal of Water Resources and Environmental Engineering,* 2 (2010) 50-59.

23. E. Ngameni, I. Tonle, J. Apohkeng, R. Bouwé, A. Jieumboué, A. Walcarius, Permselective and preconcentration properties of a surfactant-intercalated clay modified electrode, *Electroanalysis,* 18 (2006) 2243-2250. https://doi.org/10.1002/elan.200603654

24. A. Olad, Polymer/clay nanocomposites, *Advances in diverse industrial applications of nanocomposites*, (2011) 113-138.

25. E. Pehlivan, T. Altun, The study of various parameters affecting the ion exchange of Cu^{2+}, Zn^{2+}, Ni^{2+}, Cd^{2+}, and Pb^{2+} from aqueous solution on dowex 50w synthetic resin, *Journal of hazardous materials,* 134 (2006) 149-156. https://doi.org/10.1016/j.jhazmat.2005.10.052

26. X. E. Shen, X. Q. Shan, D. M. Dong, X. Y. Hua, G. Owens, Kinetics and thermodynamics of sorption of nitroaromatic compounds to as-grown and oxidized multiwalled carbon nanotubes, *Journal of colloid and interface science,* 330 (2009) 1-8. https://doi.org/10.1016/j.jcis.2008.10.023

27. S. Singh, L. Ma, M. Hendry, Characterization of aqueous lead removal by phosphatic clay: Equilibrium and kinetic studies, *Journal of hazardous materials,* 136 (2006) 654-662. https://doi.org/10.1016/j.jhazmat.2005.12.047

28. T. Thompson, M. Sobsey, J. Bartram, Providing clean water, keeping water clean: An integrated approach, *International Journal of Environmental Health Research,* 13 (2003) 89-94. https://doi.org/10.1080/0960312031000102840

29. S. Zhang, W. C. Wang, F. X. Li, J. Y. Yu, Swelling and dissolution of cellulose in NaOH aqueous solvent systems, *Cellulose Chemistry and Technology,* 47 (2013) 671-679.

(2019) ; http://www.jmaterenvironsci.com